

A facile, green, and solvent-free route to nitrogen–sulfur-codoped fluorescent carbon nanoparticles for cellular imaging†

Cite this: *RSC Adv.*, 2014, 4, 11872Received 2nd January 2014
Accepted 17th February 2014

DOI: 10.1039/c4ra00012a

www.rsc.org/advances

Hong Huang, Ya-Chun Lu, Ai-Jun Wang,* Jin-Hua Liu, Jian-Rong Chen
and Jiu-Ju Feng*

A simple, green, and solvent-free method was developed for large-scale preparation of fluorescent nitrogen–sulfur-codoped carbon nanoparticles (NSCPs) by direct thermal treatment of gentamycin sulfate at 200 °C. The as-prepared NSCPs displayed high water-solubility, long lifetime (14.01 ns), high quantum yield (27.2%), excellent stability, and low cytotoxicity, and can be used as a probe for cellular imaging.

Fluorescent carbon nanoparticles (CPs) have recently received tremendous attention due to their unique optical properties. In contrast to conventional semiconductor quantum dots (QDs) and organic dyes, the CPs are superior in the aspects of chemical stability, nonblinking fluorescence, high water solubility, good biocompatibility, and low toxicity.¹ Thus, the CPs are attractive for many applications such as sensing,² bioimaging,³ photocatalysis,⁴ and optoelectronic devices.⁵

Currently, many methods have been developed for preparation of the CPs, which are generally classified into top-down and bottom-up types.¹ For the former, the CPs are usually etched from large carbon sources by arc discharge,⁶ laser ablation,⁷ chemical oxidation,⁸ and electrochemical synthesis.⁹ For the latter, the CPs are formed from molecular precursors including microwave pyrolysis of CCl₄,¹⁰ ultrasonic treatment of glucose,¹¹ and thermal treatment of ethylenediaminetetraacetic acid.¹² Among them, thermal synthesis strategy is particularly simple and efficient.

Lately, heteroatom doping of the CPs, especially with nitrogen and/or sulfur, has demonstrated an attractive strategy to tune their electronic properties, surface and local chemistry, as well as extending their applications.¹³ Zhu *et al.* synthesized nitrogen-doped CPs (NCPs) by hydrothermal treatment of soy milk, which exhibited the improved catalytic activity for oxygen

reduction reaction.¹⁴ Chandra and coworkers synthesized sulfur-doped CPs from thiomalic acid for the fabrication of solar cells.¹⁵ Dong's group fabricated highly luminescent nitrogen–sulfur-codoped CPs (NSCPs) from a hybrid carbon source comprising L-cysteine and citric acid.¹⁶ In another study, Sun *et al.* reported the preparation of NSCPs with broad absorption bands for visible-light photocatalysis.¹⁷ More recently, Guo *et al.* constructed nitrogen–sulfur-codoped graphene by sulfate-reducing bacteria treating graphene oxide, which exhibited the improved electrochemical sensing performances of heavy metal ions, compared with single-doped graphene.¹⁸ Despite these good examples, it is still a challenge to develop simple, cost-effective and environmentally benign approaches in the synthesis of novel NSCPs.

Herein, we have developed a simple, green and solvent-free method for preparation of the NSCPs by thermal treatment of gentamycin sulfate at a relatively low temperature. For a typical synthesis, 0.1 g of gentamycin sulfate was heated in a stainless steel autoclave at 200 °C for 1.5 h, followed by dispersing the product in water and purified by filtration and centrifugation. The product (Fig. 1A) contains numerous well dispersed spherical small particles from the transmission electron microscopy (TEM) image, with an average diameter of 2.8 ± 0.7 nm (Fig. 1B) by measuring over 100 random nanoparticles. Their size is similar to that of the CPs prepared with ascorbic acid.¹⁹ High resolution TEM (HRTEM) image provides the clear lattice planes with an interfringe distance of 0.23 nm (inset in

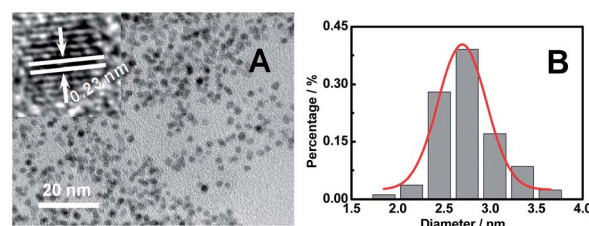


Fig. 1 TEM image (A) and the size distribution histogram (B) of the NSCPs. Inset shows HRTEM image of an individual NSCP.

College of Chemistry and Life Science, College of Geography and Environmental Science, Zhejiang Normal University, Jinhua 321004, China. E-mail: jjfeng@zjnu.cn; ajwang@zjnu.cn; Fax: +86 579 8228226; Tel: +86 579 8228226

† Electronic supplementary information (ESI) available. See DOI: 10.1039/c4ra00012a

Fig. 1A), corresponding to the (100) planes of graphite,²⁰ as strongly supported by X-ray diffraction (XRD) analysis with an intense peak at 20.1° associated with graphitic structure (Fig. S1A†). Furthermore, the interlayer spacing is calculated to be 0.44 nm, much larger than that of bulk graphite (0.34 nm). This is ascribed to the existence of abundant functional groups such as $-\text{O}-\text{H}$, $-\text{C}-\text{N}$, and $\text{C}=\text{O}$ groups.²¹

Fig. 2A shows the X-ray photoelectron spectroscopy (XPS) analysis of the NSCPs, in which there are three dominant peaks at 533.6 eV (O_{1s}), 402.5 eV (N_{1s}), and 286.5 eV (C_{1s}). Furthermore, there are two weak peaks centered at 169.8 and 232.6 eV, which are assigned to S_{2p} and S_{2s} , respectively. These results confirm the coexistence of nitrogen and sulfur elements. Specifically, the deconvolution of the C_{1s} region (Fig. 2B) shows four peaks at 287.6, 286.2, 285.5, and 284.7 eV, which are indexed to the $\text{C}=\text{N}/\text{C}=\text{O}$, $\text{C}-\text{O}$, $\text{C}-\text{N}$, and $\text{C}-\text{C}$ groups, respectively.²² In the high-resolution spectrum of N_{1s} , the peaks at 401.3, 400.5, and 399.4 eV correspond to the $\text{N}-\text{H}$, $\text{N}-(\text{C})_3$, and $\text{C}-\text{N}-\text{C}$ groups, respectively (Fig. 2C).²³ The high-resolution spectrum of S_{2p} (Fig. 2D) displays three peaks at 167.6, 168.5, and 169.3 eV, which are come from the oxidized sulfur groups, *i.e.*, $-\text{C}-\text{S}(\text{O})_x-\text{C}-$ bonds ($x = 2, 3, 4$),²⁴ different from the S atoms of the NSCPs reported in the form of $-\text{C}-\text{S}-$ bond.¹⁶

Fourier transform infrared (FT-IR) spectrum was recorded to identify the functional groups on the NSCPs (Fig. S1B†). The broad absorption bands at $3269\text{--}3463\text{ cm}^{-1}$ are assigned to the stretching vibrations of the $\text{O}-\text{H}$ and $\text{N}-\text{H}$ groups, and the band at 1602 cm^{-1} is attributed to the vibrational absorption band of $\text{C}=\text{O}$, indicating that there are many amino- and carboxyl-groups on the surface of the NSCPs.²⁵ The peaks at 2880 and 2942 cm^{-1} are attributed to the stretching vibrations of the $\text{C}-\text{H}$ bands, and the peak at 1036 cm^{-1} is originated from the symmetric stretching of the $-\text{SO}_3^-$ groups.²⁴ These results manifest effective dope of nitrogen and sulfur atoms into the NSCPs. The zeta potential is measured to be 17.6 mV, which can be attributed to the existence of N-containing groups on the surface of the NSCPs.

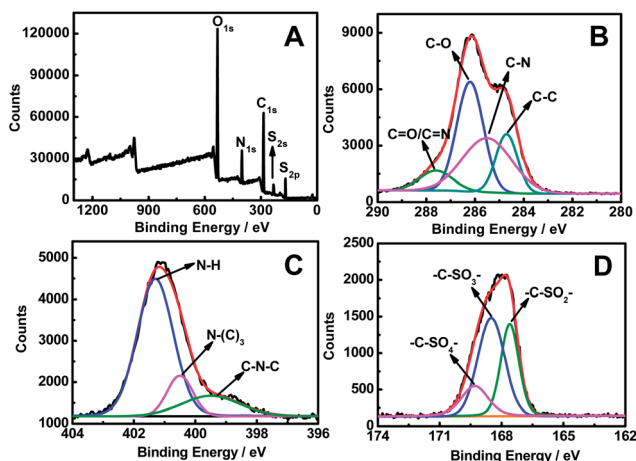


Fig. 2 XPS full scan (A), C_{1s} (B), N_{1s} (C), and S_{2p} (D) spectra of the NSCPs.

The formation of the NSCPs possibly undergoes four stages, including dehydration, polymerization, carbonization, and surface passivation.²⁶ Initially, gentamycin sulfate molecules are connected *via* an intermolecular dehydration. With the increase of reaction time, a polymerization process occurs, where gentamycin sulfate molecules are aromatized by intramolecular dehydration. The newly generated intermediates are further carbonized, inducing the formation of carbon nuclei and subsequently grow to the NSCPs with hydrophilic functional groups (*e.g.* hydroxyl groups, carboxyl groups, amino groups, and oxidized sulfur groups) on its surface, as confirmed by the XPS and FTIR data.

The NSCPs suspension is clear yellow in visible light and exhibits a bright blue fluorescence under 365 nm UV light (insets in Fig. 3A). The UV-vis absorption spectrum shows the NSCPs with two representative peaks (Fig. 3A), which is consistent with the CPs from acetic acid.²⁷ The peak at 256 nm probably originates from the formation of multiple poly-aromatic chromophores, while the peak at 300 nm may be come from $n-\pi^*$ transitions of $\text{C}=\text{O}$ groups.²⁷ Meanwhile, the maximum fluorescence peak is observed at 403 nm with a full width at half maximum of 72 nm under the excitation of 318 nm (Fig. 3A), suggesting narrow size distribution of the NSCPs, as revealed by the TEM measurements.

Varying the excitation wavelength from 320 to 500 nm causes gradually red shift of the emission peak from 410 to 538 nm, accompanied with the decrease of the fluorescence intensity (Fig. 3B and S1C†), suggesting that the fluorescence of the NSCPs is strongly dependent on the excitation wavelength. The excitation dependent feature has been extensively reported in fluorescent CPs previously, which is attributed to the difference in particle size and a distribution of different emissive trap sites of the CPs.^{21,28} Additionally, the corresponding fluorescence lifetime is around 14.01 ns, with excitation and emission wavelength of 318 and 403 nm, respectively (Fig. S1D†). This value is higher than most of the reported CPs,²⁹ and will be beneficial for their applications in lifetime-based imaging and sensing, because it is independent of fluorophore concentration and excitation intensity.³⁰

Using quinine sulfate (54% in 0.1 M H_2SO_4) as a standard, the quantum yield of the NSCPs is about 27.2%, which is higher than that of the NCPs (16.9%) derived from gentamycin, but lower than that of the NSCPs reported by Dong and coworkers.¹⁶ This

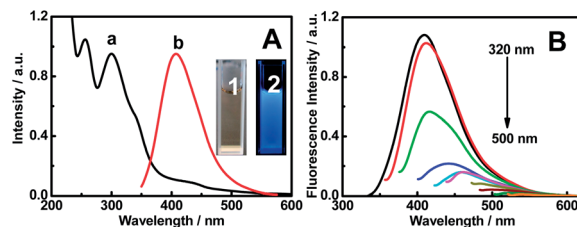


Fig. 3 (A) UV-vis absorption (curve a) and fluorescence (curve b) spectra of the NSCPs. Insets show the photographs taken under visible light (1) and UV light (2). (B) Fluorescence emission spectra obtained at different excitation wavelengths with 20 nm increments from 320 to 500 nm.

is probably due to the fact that the codoped sulfur atoms would improve the effects of nitrogen atoms on the properties of the doped CPs through the synergy effects. Furthermore, the quantum yield here is lower than that in the form of C–S–bond (70% at least),¹⁶ because the valence state is higher, mainly present in oxidized sulfur groups. In fact, the CPs prepared from gentamycin and gentamycin sulfate display similar optical properties. Under excitation of 318 nm, the maximum emission wavelength of the NCPs is 405 nm, almost identical to the NSCPs (Fig. S2A†). Both the CPs exhibit excitation-dependent properties (Fig. 3B and S2B†) and similar lifetime (*ca.* 14 ns, Fig. S1D†). These results suggest that the two CPs may have the similar fluorescence nature.

The fluorescence intensity of the NSCPs almost remains constant in various NaCl concentrations (up to 0.5 M), revealing good stability of the NSCPs in high ionic strength environment (Fig. S3A†). Meanwhile, only a slight change in the fluorescence intensity is observed after irradiation for 7 h with a 500 W Xe lamp (Fig. S3B†). Similarly, without any precipitates or the loss of fluorescence is noticed as the NSCPs suspension is stored for 2.5 months in air at room temperature (Fig. S3C†), further implying their excellent stability. Interestingly, it is found that the fluorescence intensity is decreased by increasing the pH values in the present system, indicating the possibility of constructing a potential pH sensor (Fig. S3D†). All these fascinating properties reveal the great potential of the NSCPs for practical applications in pH sensor, bio-labelling, and bio-imaging.

For future biological applications, the inherent cytotoxicity of the NSCPs was checked with HeLa cells through the MTT assay. The cell viabilities of HeLa cells were investigated upon exposure to the NSCPs suspension with different concentrations (Fig. 4). There is no reduction in viability after incubation with high concentrations of the NSCPs even up to $100\ \mu\text{g mL}^{-1}$, suggesting their low cytotoxicity and good biocompatibility.

Using the NSCPs as a probe, the NSCPs uptake and bio-imaging experiments were *in vitro* conducted by the confocal fluorescence microscope. As expected, HeLa cells treated by the NSCPs ($20\ \mu\text{g mL}^{-1}$) become quite bright, showing blue, green, and red color by exciting at the wavelength of 405 nm, 488 nm,

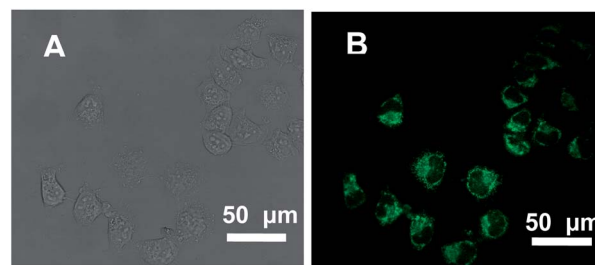


Fig. 5 Images of NSCPs incubated HeLa cells obtained under bright field (A) and excitation wavelength of 488 nm (B). The concentration of the NSCPs is $20\ \mu\text{g mL}^{-1}$.

and 543 nm, respectively, while no visible fluorescence is detected in the untreated control group under the same conditions (Fig. 5 and S4†). Importantly, the photoluminescence can only be detected in the cell membrane and cytoplasmic area, rather than in the nucleus of the cells, which would avoid genetic disruption, consistent with the finding reported by Chen and coworkers.³¹ All these results confirm the NSCPs as a promising alternative to QDs in bioimaging.

In summary, a simple, facile, green, and solvent-free method was developed in the large-scale synthesis of the NSCPs with high quantum yield (27.2%), long lifetime (14.01 ns), good water-solubility, low cytotoxicity, and excellent stability. Further studies show that the NSCPs can be used as a fluorescent probe for cellular imaging.

Acknowledgements

This work was financially supported by the NSFC (no. 21175118, 21275130, 21275131 and 21345006), and Zhejiang province university young academic leaders of academic climbing project (no. pd2013055).

Notes and references

- (a) C. Ding, A. Zhu and Y. Tian, *Acc. Chem. Res.*, 2014, **47**, 20–30; (b) H. Li, Z. Kang, Y. Liu and S.-T. Lee, *J. Mater. Chem.*, 2012, **22**, 24230–24253.
- (a) Y. Dong, R. Wang, G. Li, C. Chen, Y. Chi and G. Chen, *Anal. Chem.*, 2012, **84**, 6220–6224; (b) H. Huang, J.-J. Lv, D.-L. Zhou, N. Bao, Y. Xu, A.-J. Wang and J.-J. Feng, *RSC Adv.*, 2013, **3**, 21691–21696; (c) A. Zhu, Q. Qu, X. Shao, B. Kong and Y. Tian, *Angew. Chem.*, 2012, **124**, 7297–7301; (d) Q. Qu, A. Zhu, X. Shao, G. Shi and Y. Tian, *Chem. Commun.*, 2012, **48**, 5473–5475.
- (a) S. Sahu, B. Behera, T. K. Maiti and S. Mohapatra, *Chem. Commun.*, 2012, **48**, 8835–8837; (b) H. Huang, Y. Xu, C.-J. Tang, J. Chen, A.-J. Wang and J.-J. Feng, *New J. Chem.*, 2014, **38**, 784–789; (c) Y. Dong, C. Chen, X. Zheng, L. Gao, Z. Cui, H. Yang, C. Guo, Y. Chi and C. M. Li, *J. Mater. Chem.*, 2012, **22**, 8764–8766; (d) B. Kong, A. Zhu, C. Ding, X. Zhao, B. Li and Y. Tian, *Adv. Mater.*, 2012, **24**, 5844–5848.
- (a) H. Li, X. He, Z. Kang, H. Huang, Y. Liu, J. Liu, S. Lian, C. H. A. Tsang, X. Yang and S.-T. Lee, *Angew. Chem., Int.*

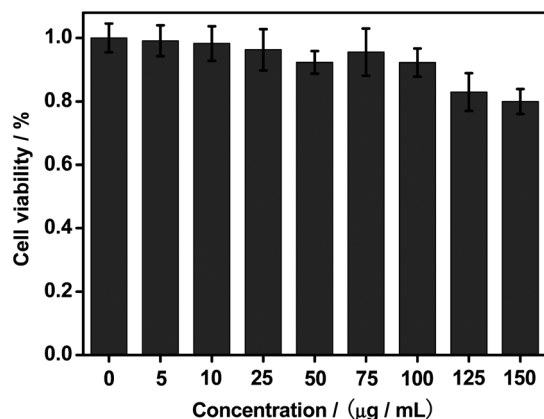


Fig. 4 Viability of HeLa cells after incubation of 24 h with different concentrations of the NSCPs, as determined by the MTT assay.

- Ed.*, 2010, **49**, 4430–4434; (b) H. Li, R. Liu, S. Lian, Y. Liu, H. Huang and Z. Kang, *Nanoscale*, 2013, **5**, 3289–3297.
- 5 (a) X. Guo, C.-F. Wang, Z.-Y. Yu, L. Chen and S. Chen, *Chem. Commun.*, 2012, **48**, 2692–2694; (b) W. Kwon, G. Lee, S. Do, T. Joo and S.-W. Rhee, *Small*, 2014, **10**, 506–513.
- 6 X. Xu, R. Ray, Y. Gu, H. J. Ploehn, L. Gearheart, K. Raker and W. A. Scrivens, *J. Am. Chem. Soc.*, 2004, **126**, 12736–12737.
- 7 S.-L. Hu, K.-Y. Niu, J. Sun, J. Yang, N.-Q. Zhao and X.-W. Du, *J. Mater. Chem.*, 2009, **19**, 484–488.
- 8 J. Shen, Y. Zhu, C. Chen, X. Yang and C. Li, *Chem. Commun.*, 2011, **47**, 2580–2582.
- 9 L. Zheng, Y. Chi, Y. Dong, J. Lin and B. Wang, *J. Am. Chem. Soc.*, 2009, **131**, 4564–4565.
- 10 S. Liu, J. Tian, L. Wang, Y. Luo, J. Zhai and X. Sun, *J. Mater. Chem.*, 2011, **21**, 11726–11729.
- 11 H. Li, X. He, Y. Liu, H. Huang, S. Lian, S.-T. Lee and Z. Kang, *Carbon*, 2011, **49**, 605–609.
- 12 D. Pan, J. Zhang, Z. Li, C. Wu, X. Yan and M. Wu, *Chem. Commun.*, 2010, **46**, 3681–3683.
- 13 (a) Y. Li, Y. Zhao, H. Cheng, Y. Hu, G. Shi, L. Dai and L. Qu, *J. Am. Chem. Soc.*, 2012, **134**, 15–18; (b) M. Zheng, Z. Xie, D. Qu, D. Li, P. Du, X. Jing and Z. Sun, *ACS Appl. Mater. Interfaces*, 2013, **5**, 13242–13247; (c) H. Tetsuka, R. Asahi, A. Nagoya, K. Okamoto, I. Tajima, R. Ohta and A. Okamoto, *Adv. Mater.*, 2012, **24**, 5333–5338; (d) Q. Liu, B. Guo, Z. Rao, B. Zhang and J. R. Gong, *Nano Lett.*, 2013, **13**, 2436–2441.
- 14 C. Zhu, J. Zhai and S. Dong, *Chem. Commun.*, 2012, **48**, 9367–9369.
- 15 S. Chandra, P. Patra, S. H. Pathan, S. Roy, S. Mitra, A. Layek, R. Bhar, P. Pramanik and A. Goswami, *J. Mater. Chem. B*, 2013, **1**, 2375–2382.
- 16 Y. Dong, H. Pang, H. B. Yang, C. Guo, J. Shao, Y. Chi, C. M. Li and T. Yu, *Angew. Chem., Int. Ed.*, 2013, **52**, 7800–7804.
- 17 D. Qu, M. Zheng, P. Du, Y. Zhou, L. Zhang, D. Li, H. Tan, Z. Zhao, Z. Xie and Z. Sun, *Nanoscale*, 2013, **5**, 12272–12277.
- 18 P. Guo, F. Xiao, Q. Liu, H. Liu, Y. Guo, J. R. Gong, S. Wang and Y. Liu, *Sci. Rep.*, 2013, **3**, DOI: 10.1038/srep03499.
- 19 X. Jia, J. Li and E. Wang, *Nanoscale*, 2012, **4**, 5572–5575.
- 20 X. Zhang, F. Wang, H. Huang, H. Li, X. Han, Y. Liu and Z. Kang, *Nanoscale*, 2013, **5**, 2274–2278.
- 21 L. Tang, R. Ji, X. Cao, J. Lin, H. Jiang, X. Li, K. S. Teng, C. M. Luk, S. Zeng, J. Hao and S. P. Lau, *ACS Nano*, 2012, **6**, 5102–5110.
- 22 S. Liu, J. Tian, L. Wang, Y. Zhang, X. Qin, Y. Luo, A. M. Asiri, A. O. Al-Youbi and X. Sun, *Adv. Mater.*, 2012, **24**, 2037–2041.
- 23 W. Lu, X. Qin, S. Liu, G. Chang, Y. Zhang, Y. Luo, A. M. Asiri, A. O. Al-Youbi and X. Sun, *Anal. Chem.*, 2012, **84**, 5351–5357.
- 24 D. Sun, R. Ban, P.-H. Zhang, G.-H. Wu, J.-R. Zhang and J.-J. Zhu, *Carbon*, 2013, **64**, 424–434.
- 25 W. Li, Z. Zhang, B. Kong, S. Feng, J. Wang, L. Wang, J. Yang, F. Zhang, P. Wu and D. Zhao, *Angew. Chem., Int. Ed.*, 2013, **52**, 8151–8155.
- 26 (a) Z. Yang, M. Xu, Y. Liu, F. He, F. Gao, Y. Su, H. Wei and Y. Zhang, *Nanoscale*, 2014, **6**, 1890–1895; (b) P.-C. Hsu and H.-T. Chang, *Chem. Commun.*, 2012, **48**, 3984–3986; (c) Z.-C. Yang, X. Li and J. Wang, *Carbon*, 2011, **49**, 5207–5212.
- 27 Y. Fang, S. Guo, D. Li, C. Zhu, W. Ren, S. Dong and E. Wang, *ACS Nano*, 2011, **6**, 400–409.
- 28 (a) Y.-P. Sun, B. Zhou, Y. Lin, W. Wang, K. A. S. Fernando, P. Pathak, M. J. Mezziani, B. A. Harruff, X. Wang, H. Wang, P. G. Luo, H. Yang, M. E. Kose, B. Chen, L. M. Veca and S.-Y. Xie, *J. Am. Chem. Soc.*, 2006, **128**, 7756–7757; (b) P. Yu, X. Wen, Y.-R. Toh and J. Tang, *J. Phys. Chem. C*, 2012, **116**, 25552–25557.
- 29 (a) H. Li, H. Ming, Y. Liu, H. Yu, X. He, H. Huang, K. Pan, Z. Kang and S.-T. Lee, *New J. Chem.*, 2011, **35**, 2666–2670; (b) Z. L. Wu, P. Zhang, M. X. Gao, C. F. Liu, W. Wang, F. Leng and C. Z. Huang, *J. Mater. Chem. B*, 2013, **1**, 2868–2873.
- 30 (a) L. Shang, N. Azadfar, F. Stockmar, W. Send, V. Trouillet, M. Bruns, D. Gerthsen and G. U. Nienhaus, *Small*, 2011, **7**, 2614–2620; (b) L. Shang, F. Stockmar, N. Azadfar and G. U. Nienhaus, *Angew. Chem., Int. Ed.*, 2013, **52**, 1115–11157.
- 31 B. Chen, F. Li, S. Li, W. Weng, H. Guo, T. Guo, X. Zhang, Y. Chen, T. Huang, X. Hong, S. You, Y. Lin, K. Zeng and S. Chen, *Nanoscale*, 2013, **5**, 1967–1971.